Spin-dependent current noises in transport through coupled quantum dots

2008 J. Phys.: Condens. Matter 20 345215

(http://iopscience.iop.org/0953-8984/20/34/345215)

J. Phys.: Condens. Matter **20** (2008) 345215 (7pp) doi:10.1088/0953-8984/20/34/345215

Spin-dependent current noises in transport through coupled quantum dots

JunYan Luo[1,2], Xin-Qi Li[1,2] and YiJing Yan[2]

[1] State Key Laboratory for Superlattices and Microstructures, Institute of Semiconductors, Chinese Academy of Sciences, PO Box 912, Beijing 100083, People's Republic of China
[2] Department of Chemistry, Hong Kong University of Science and Technology, Kowloon, Hong Kong

Received 15 February 2008, in final form 11 July 2008
Published 1 August 2008
Online at stacks.iop.org/JPhysCM/20/345215

Abstract
Current fluctuations can provide additional insight into quantum transport in mesoscopic systems. The present work is carried out for the fluctuation properties of transport through a pair of coupled quantum dots which are connected with ferromagnetic electrodes. Based on an efficient particle-number-resolved master equation approach, we are concerned with not only fluctuations of the total charge and spin currents, but also of each individual spin-dependent component. As a result of competition among the spin polarization, Coulomb interaction, and dot–dot tunnel coupling, rich behaviors are found for the self- and mutual-correlation functions of the spin-dependent currents.

1. Introduction

Noise from transport current through mesoscopic systems can provide useful information beyond the average current [1, 2]. Typical examples include quantum shuttles [3–6], spin valves [7–9], double-dot structures [10–13], as well as qubit measurement [14–17]. These studies were focused largely on the total charge current. A relatively less exploited subject, but now gaining increasing attention, is the spin-dependent current fluctuations [18–21]. A number of interesting examples are listed as follows. (i) It was shown in [18] that the shot noise of spin current is closely related to the spin unit of quasiparticles. (ii) In the absence of charge current, the magnetically pumped spin current noise through quantum dots in the Coulomb blockade regime can serve as a sensitive probe of spin decoherence [19]. (iii) For a quantum dot strongly coupled to a cavity field, the shot noise of the spin current exhibits the clear signature of the discrete nature of the photon states [20]. (iv) Spin-dependent shot noise of unpolarized currents can be used to detect attractive or repulsive correlations [21].

In this work we study the spin-dependent current noises for transport through a pair of coupled quantum dots connected with ferromagnetic (FM) electrodes. Owing to the additional modulation of the dot–dot coupling, rich noise behaviors are found as a consequence of the interplay between the Coulomb correlation and the spin polarization of the FM electrodes. Methodologically, we employ an efficient particle-number-resolved master equation approach [15, 24, 25], with proper extension by including the spin degrees of freedom. This approach, which can be considered as a finite temperature and voltage extension of the 'n'-resolved quantum Bloch-type equation proposed by Gurvitz and Prager [26], has the advantages of its simplicity of treating properly a broad range of dissipation, as well as its transparency in the involved dynamics and many-body interactions.

This paper is organized as follows. We begin in section 2 with the model set-up of double dots connected with FM electrodes. We then present in section 3 a general formalism for both the spin-dependent currents and their noises. Numerical results are presented in sections 4 and 5, and they are then followed by the conclusion in section 6.

2. Model description

The system under study is schematically shown in figure 1. The left and right quantum dots are labeled by 'L' and 'R', respectively. The total Hamiltonian contains three parts:

$$\hat{H} = \hat{H}_{\rm B} + \hat{H}_{\rm S} + \hat{H}'. \tag{1}$$

$\hat{H}_{\rm B} = \sum_{\alpha={\rm L,R}} \sum_{k,\sigma} \varepsilon_{\alpha k} c^{\dagger}_{\alpha k\sigma} c_{\alpha k\sigma}$ describes the left and right electrodes, which are magnetically polarized. $c_{\alpha k\sigma}$ ($c^{\dagger}_{\alpha k\sigma}$) is the electron annihilation (creation) operator of the electrode α = L or R, with spin $\sigma = \uparrow$ or $\downarrow$. The FM electrodes are characterized by the spin-dependent density of states $g_{\alpha\sigma}(\omega)$.

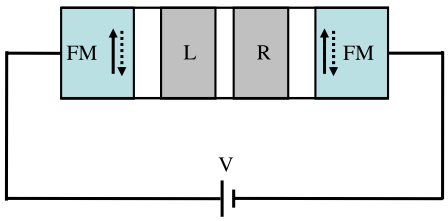

Figure 1. Schematic set-up for transport through a pair of coupled quantum dots connected with ferromagnetic electrodes.
(This figure is in colour only in the electronic version)

Moreover, the densities of the states are assumed to be energy-independent, i.e. $g_{\alpha\sigma}(\omega) = g_{\alpha\sigma}$. Then, the FM polarization of the electrodes is simply determined by a parameter $p_\alpha = (g_{\alpha\uparrow} - g_{\alpha\downarrow})/(g_{\alpha\uparrow} + g_{\alpha\downarrow})$, which satisfies $-1 \leqslant p_\alpha \leqslant 1$.

The second Hamiltonian is for the coupled dots:

$$\hat{H}_{\rm S} = \sum_{\alpha={\rm L,R}} E_\alpha \hat{n}_\alpha + U_0(\hat{n}_{\rm L\uparrow}\hat{n}_{\rm L\downarrow} + \hat{n}_{\rm R\uparrow}\hat{n}_{\rm R\downarrow}) + U'\hat{n}_{\rm L}\hat{n}_{\rm R} + \Omega\sum_\sigma (d^\dagger_{{\rm L}\sigma} d_{{\rm R}\sigma} + d^\dagger_{{\rm R}\sigma} d_{{\rm L}\sigma}). \quad (2)$$

Here $\hat{n}_{\alpha\sigma} = d^\dagger_{\alpha\sigma} d_{\alpha\sigma}$ and $\hat{n}_\alpha = \sum_\sigma \hat{n}_{\alpha\sigma}$, with $d_{\alpha\sigma}$ ($d^\dagger_{\alpha\sigma}$) the electron annihilation (creation) operator in the quantum dot α and with spin σ. Note that here α labels the left and right quantum dots rather than the electrodes. Each quantum dot is assumed to have only one spin-degenerate energy level $E_{\rm L/R}$. U_0 and U' are the intradot and interdot Coulomb interactions, and Ω is the coupling strength of the two dots. The typical value of the intradot interaction U_0 is estimated to be 4–5 meV and $U' \approx U_0/2$ [22].

The third Hamiltonian describes the coupling of the central dots to the electrodes, in terms of $\hat{H}' = \sum_{\alpha k\sigma}(t_{\alpha k} c^\dagger_{\alpha k\sigma} d_{\alpha\sigma} + {\rm H.c.})$. Note that, due to spin polarization of the electrodes, the tunnel coupling strength would become spin-dependent, i.e. with $\Gamma_{\alpha\uparrow} = (1 + p_\alpha)\Gamma_\alpha/2$ differing from $\Gamma_{\alpha\downarrow} = (1 - p_\alpha)\Gamma_\alpha/2$, where $\Gamma_\alpha = 2\pi \sum_k |t_{\alpha k}|^2 \delta(\varepsilon_{\alpha k} - \omega)$ is the total coupling strength regardless of the spin orientation, and is estimated to be 10^9–10^{10} s^{-1} [23].

In this work, corresponding to different bias voltages, we will *effectively* consider the following three cases. Case (i): noninteracting (NINT) dots, i.e. each dot can be doubly occupied. Case (ii): single-dot Coulomb blockade (SDCB). In this case double occupation on the same dot is prohibited, but each of the two dots can hold an electron. Case (iii): double-dot Coulomb blockade (DDCB). In this case, there is at most only one electron in the two dots. Experimentally, the above-mentioned different cases can be achieved by appropriately adjusting the applied bias voltage with respect to the intradot and interdot charging energies [25].

3. Formalism

In this section we outline the master equation approach for the calculation of the spin-dependent shot noise. The main point is to obtain the equation of motion for the *conditional* reduced density matrix of the central quantum dots, which is conditioned not only on the transmitted electron numbers, but also on their spins.

3.1. Electron-number-resolved master equation

To achieve the description of spin-dependent transport, we will first extend the 'n'-resolved quantum master equation [15, 24, 25] to include spin degrees of freedom. Let us start with the reduced density matrix, defined as $\rho(t) \equiv {\rm Tr_B}[\rho_{\rm T}(t)]$, i.e. tracing over the electrode states from the total density matrix. Assuming the tunneling Hamiltonian $\hat{H}'$ is weak, the second-order cumulant expansion leads to the master equation [27]

$$\dot{\rho}(t) = -{\rm i}\mathcal{L}\rho(t) - \int_0^\infty {\rm d}\tau \langle \mathcal{L}'(t)\mathcal{G}(t,\tau)\mathcal{L}'(\tau)\mathcal{G}^\dagger(t,\tau)\rangle \rho(t), \quad (3)$$

where the Liouvillian superoperators are defined as $\mathcal{L}A \equiv [\hat{H}_{\rm S}, A]$, $\mathcal{L}'A \equiv [\hat{H}', A]$ and $\mathcal{G}(t,\tau)A \equiv G(t,\tau)AG^\dagger(t,\tau)$, with $G(t,\tau)$ the usual propagator associated with the system Hamiltonian $\hat{H}_{\rm S}$.

To condition the master equation on the electron number transmitted [15, 24, 25], we decompose the entire Hilbert space B of the left and right electrodes into the sum of the subspaces, $\mathrm{B}_{\rm L}^{(n_{\rm L\uparrow}, n_{\rm L\downarrow})} \otimes \mathrm{B}_{\rm R}^{(n_{\rm R\uparrow}, n_{\rm R\downarrow})}$, where $n_{\alpha\sigma}$ is the number of electrons with spin-σ arriving at the electrode α (α = L or R). Partially tracing over states in each subspace leads to the spin-resolved quantum master equation for the reduced density matrix:

$$\begin{aligned}\dot{\rho}^{\binom{n_{\rm L\uparrow}, n_{\rm R\uparrow}}{n_{\rm L\downarrow}, n_{\rm R\downarrow}}} = {} & -{\rm i}\mathcal{L}\rho^{\binom{n_{\rm L\uparrow}, n_{\rm R\uparrow}}{n_{\rm L\downarrow}, n_{\rm R\downarrow}}} - \tfrac{1}{2}\Big\{\sum_{\alpha\sigma}\big[d^\dagger_{\alpha\sigma} A^{(-)}_{\alpha\sigma}\rho^{\binom{n_{\rm L\uparrow}, n_{\rm R\uparrow}}{n_{\rm L\downarrow}, n_{\rm R\downarrow}}} \\ & + \rho^{\binom{n_{\rm L\uparrow}, n_{\rm R\uparrow}}{n_{\rm L\downarrow}, n_{\rm R\downarrow}}} A^{(+)}_{\alpha\sigma} d^\dagger_{\alpha\sigma}\big] - \big[d^\dagger_{\rm L\uparrow}\rho^{\binom{n_{\rm L\uparrow}+1, n_{\rm R\uparrow}}{n_{\rm L\downarrow}, n_{\rm R\downarrow}}} A^{(+)}_{\rm L\uparrow} \\ & + d^\dagger_{\rm L\downarrow}\rho^{\binom{n_{\rm L\uparrow}, n_{\rm R\uparrow}}{n_{\rm L\downarrow}+1, n_{\rm R\downarrow}}} A^{(+)}_{\rm L\downarrow} + A^{(-)}_{\rm L\uparrow}\rho^{\binom{n_{\rm L\uparrow}-1, n_{\rm R\uparrow}}{n_{\rm L\downarrow}, n_{\rm R\downarrow}}} d^\dagger_{\rm L\uparrow} \\ & + A^{(-)}_{\rm L\downarrow}\rho^{\binom{n_{\rm L\uparrow}, n_{\rm R\uparrow}}{n_{\rm L\downarrow}-1, n_{\rm R\downarrow}}} d^\dagger_{\rm L\downarrow} + d^\dagger_{\rm R\uparrow}\rho^{\binom{n_{\rm L\uparrow}, n_{\rm R\uparrow}+1}{n_{\rm L\downarrow}, n_{\rm R\downarrow}}} A^{(+)}_{\rm R\uparrow} \\ & + d^\dagger_{\rm R\downarrow}\rho^{\binom{n_{\rm L\uparrow}, n_{\rm R\uparrow}}{n_{\rm L\downarrow}, n_{\rm R\downarrow}+1}} A^{(+)}_{\rm R\downarrow} + A^{(-)}_{\rm R\uparrow}\rho^{\binom{n_{\rm L\uparrow}, n_{\rm R\uparrow}-1}{n_{\rm L\downarrow}, n_{\rm R\downarrow}}} d^\dagger_{\rm R\uparrow} \\ & + A^{(-)}_{\rm R\downarrow}\rho^{\binom{n_{\rm L\uparrow}, n_{\rm R\uparrow}}{n_{\rm L\downarrow}, n_{\rm R\downarrow}-1}} d^\dagger_{\rm R\downarrow}\big] + {\rm H.c.}\Big\}. \end{aligned} \quad (4)$$

Here, $A^{(+)}_{\alpha\sigma} \equiv \sum_{\sigma'} C^{(+)}_{\alpha\sigma'\sigma}(\mathcal{L}) d_{\alpha\sigma'}$ and $A^{(-)}_{\alpha\sigma} \equiv \sum_{\sigma'} C^{(-)}_{\alpha\sigma\sigma'}(-\mathcal{L}) d_{\alpha\sigma'}$, with $C^{(\pm)}_{\alpha\sigma\sigma'}(\pm\mathcal{L}) = \int {\rm d}t C^{(\pm)}_{\alpha\sigma\sigma'}(t){\rm e}^{\pm{\rm i}\mathcal{L}t}$. The involved bath correlation functions are defined as $C^{(+)}_{\alpha\sigma\sigma'}(t-\tau) \equiv \langle f^\dagger_{\alpha\sigma}(t) f_{\alpha\sigma'}(\tau)\rangle$ and $C^{(-)}_{\alpha\sigma\sigma'}(t-\tau) \equiv \langle f_{\alpha\sigma}(t) f^\dagger_{\alpha\sigma'}(\tau)\rangle$, with $f_{\alpha\sigma} = \sum_k t_{\alpha\sigma} c_{\alpha k\sigma}$ and $\langle\cdots\rangle \equiv {\rm Tr_B}[(\cdots)\rho_{\rm B}]$ standing for the usual meaning of thermal bath average.

3.2. Spin-dependent currents

With the knowledge of the above conditional state, the joint probability distribution function is obtained as $P[\binom{n_{\rm L\uparrow}, n_{\rm R\uparrow}}{n_{\rm L\downarrow}, n_{\rm R\downarrow}}, t] \equiv {\rm Tr}\,\rho^{\binom{n_{\rm L\uparrow}, n_{\rm R\uparrow}}{n_{\rm L\downarrow}, n_{\rm R\downarrow}}}$, where ${\rm Tr}(\cdots)$ denotes the trace over the system states. It allows us to evaluate the spin-σ-dependent current through the junction α by

$$I^\sigma_\alpha = e\frac{\rm d}{{\rm d}t}\sum_{n_{\rm L\uparrow}, n_{\rm L\downarrow}}\sum_{n_{\rm R\uparrow}, n_{\rm R\downarrow}} n_{\alpha\sigma} P\left[\binom{n_{\rm L\uparrow}, n_{\rm R\uparrow}}{n_{\rm L\downarrow}, n_{\rm R\downarrow}}, t\right] = e\,{\rm Tr}\,\dot{N}^\sigma_\alpha, \quad (5)$$

Table 1. Spin-dependent currents, as well as the total charge and spin currents, for the (i) NINT case, (ii) SDCB case and (iii) DDCB case, respectively. Here, $\gamma_0 \equiv \Gamma_L + \Gamma_R$, $\gamma_s \equiv 2\Gamma_L + \Gamma_R$ and $\gamma_d \equiv 4\Gamma_L + \Gamma_R$ are the corresponding total effective tunneling rates for these three cases.

Cases	(i)	(ii)	(iii)
$\bar{I}^{\uparrow}/e$	$(1+p)\frac{\Gamma_L\Gamma_R\Omega^2/\gamma_0}{\Omega^2+\frac{1}{4}(1+p)^2\Gamma_L\Gamma_R}$	$\frac{1+p}{2}\frac{2\Gamma_L\Gamma_R\Omega^2/\gamma_s}{\Omega^2+\frac{1}{2}(1+p^2\Gamma_R/\gamma_s)\Gamma_L\Gamma_R}$	$\frac{1+p}{2}\frac{4\Gamma_L\Gamma_R\Omega^2/\gamma_d}{2\Omega^2+(1+p^2)(\Gamma_L\Gamma_R^2/\gamma_d)}$
$\bar{I}^{\downarrow}/e$	$(1-p)\frac{\Gamma_L\Gamma_R\Omega^2/\gamma_0}{\Omega^2+\frac{1}{4}(1-p)^2\Gamma_L\Gamma_R}$	$\frac{1-p}{2}\frac{2\Gamma_L\Gamma_R\Omega^2/\gamma_s}{\Omega^2+\frac{1}{2}(1+p^2\Gamma_R/\gamma_s)\Gamma_L\Gamma_R}$	$\frac{1-p}{2}\frac{4\Gamma_L\Gamma_R\Omega^2/\gamma_d}{2\Omega^2+(1+p^2)(\Gamma_L\Gamma_R^2/\gamma_d)}$
$\bar{I}^{\rm ch}/e$	$\frac{8\Gamma_L\Gamma_R\Omega^2[(1-p^2)\Gamma_L\Gamma_R+4\Omega^2]/\gamma_0}{[(1+p^2)\Gamma_L\Gamma_R+4\Omega^2]^2-4p^2\Gamma_L^2\Gamma_R^2}$	$\frac{2\Gamma_L\Gamma_R\Omega^2/\gamma_s}{\Omega^2+\frac{1}{2}(1+p^2\Gamma_R/\gamma_s)\Gamma_L\Gamma_R}$	$\frac{4\Gamma_L\Gamma_R\Omega^2/\gamma_d}{2\Omega^2+(1+p^2)(\Gamma_L\Gamma_R^2/\gamma_d)}$
$\bar{I}^{\rm sp}/e$	$p\frac{8\Gamma_L\Gamma_R\Omega^2[(p^2-1)\Gamma_L\Gamma_R+4\Omega^2]/\gamma_0}{[(1+p^2)\Gamma_L\Gamma_R+4\Omega^2]^2-4p^2\Gamma_L^2\Gamma_R^2}$	$p\frac{2\Gamma_L\Gamma_R\Omega^2/\gamma_s}{\Omega^2+\frac{1}{2}(1+p^2\Gamma_R/\gamma_s)\Gamma_L\Gamma_R}$	$p\frac{4\Gamma_L\Gamma_R\Omega^2/\gamma_d}{2\Omega^2+(1+p^2)(\Gamma_L\Gamma_R^2/\gamma_d)}$

where $N_\alpha^\sigma \equiv \sum_{n_{L\uparrow},n_{L\downarrow},n_{R\uparrow},n_{R\downarrow}} n_{\alpha\sigma}\rho^{\binom{n_{L\uparrow},n_{R\uparrow}}{n_{L\downarrow},n_{R\downarrow}}}$. Based on (4), we obtain

$$\frac{\mathrm{d}}{\mathrm{d}t}N_\alpha^\sigma = -\mathrm{i}\mathcal{L}N_\alpha^\sigma - \frac{1}{2}\Big\{\sum_{\alpha'\sigma'}\big[d_{\alpha'\sigma'}^\dagger, A_{\alpha'\sigma'}^{(-)}N_\alpha^\sigma - N_\alpha^\sigma A_{\alpha'\sigma'}^{(+)}\big] + \big[d_{\alpha\sigma}^\dagger\rho(t)A_{\alpha\sigma}^{(+)} - A_{\alpha\sigma}^{(-)}\rho(t)d_{\alpha\sigma}^\dagger\big] + \mathrm{H.c.}\Big\}. \tag{6}$$

This leads to

$$I_\alpha^\sigma = \tfrac{1}{2}e\,\mathrm{Tr}\big\{\big[d_{\alpha\sigma}^\dagger A_{\alpha\sigma}^{(-)} - A_{\alpha\sigma}^{(+)}d_{\alpha\sigma}^\dagger\big]\rho(t) + \mathrm{H.c.}\big\}, \tag{7}$$

where $\rho(t)$ is the unconditional density matrix that satisfies (3), or

$$\dot{\rho}(t) = -\mathrm{i}\mathcal{L}\rho(t) - \tfrac{1}{2}\sum_{\alpha\sigma}\big\{\big[d_{\alpha\sigma}^\dagger, A_{\alpha\sigma}^{(-)}\rho(t) - \rho(t)A_{\alpha\sigma}^{(+)}\big] + \mathrm{H.c.}\big\}. \tag{8}$$

3.3. Spin-dependent noises

Note that the total charge and spin currents through junction α are $I_\alpha^{\rm ch} = I_\alpha^\uparrow + I_\alpha^\downarrow$ and $I_\alpha^{\rm sp} = I_\alpha^\uparrow - I_\alpha^\downarrow$. The total charge current noise and spin current noise can then be expressed as

$$S_{\alpha\alpha'}^{\rm ch} = S_{\alpha\alpha'}^{\uparrow\uparrow} + S_{\alpha\alpha'}^{\downarrow\downarrow} + S_{\alpha\alpha'}^{\uparrow\downarrow} + S_{\alpha\alpha'}^{\downarrow\uparrow}, \tag{9a}$$

$$S_{\alpha\alpha'}^{\rm sp} = S_{\alpha\alpha'}^{\uparrow\uparrow} + S_{\alpha\alpha'}^{\downarrow\downarrow} - S_{\alpha\alpha'}^{\uparrow\downarrow} - S_{\alpha\alpha'}^{\downarrow\uparrow}, \tag{9b}$$

where the individual spin-dependent noise spectrum is defined as $S_{\alpha\alpha'}^{\sigma\sigma'}(\omega) \equiv \int_{-\infty}^{\infty}\mathrm{d}t\cos(\omega t)\langle\{\Delta I_\alpha^\sigma(t), \Delta I_{\alpha'}^{\sigma'}(0)\}\rangle$, with $\Delta I_\alpha^\sigma(t) \equiv I_\alpha^\sigma(t) - \bar{I}_\alpha^\sigma$. In the following, fluctuation between the same or opposite spin currents is referred to as self- or mutual-correlation shot noise, respectively. Based on the MacDonald's formula [28, 6, 29], it follows that

$$S_{\alpha\alpha'}^{\sigma\sigma'}(\omega) = 2\omega\int_0^\infty \mathrm{d}t\,\sin(\omega t)\frac{\mathrm{d}}{\mathrm{d}t}\big[M_{\alpha\alpha'}^{\sigma\sigma'}(t) - \bar{I}_\alpha^\sigma\bar{I}_{\alpha'}^{\sigma'}t^2\big], \tag{10}$$

where $\bar{I}_\alpha^\sigma$ is the stationary current obtained from (8) and $M_{\alpha\alpha'}^{\sigma\sigma'}(t) \equiv e^2\sum_{n_{L\uparrow},n_{L\downarrow},n_{R\uparrow},n_{R\downarrow}} n_{\alpha\sigma}n_{\alpha'\sigma'}P[\binom{n_{L\uparrow},n_{R\uparrow}}{n_{L\downarrow},n_{R\downarrow}}, t]$. Using the spin-resolved master equation (4), one finds

$$\frac{\mathrm{d}}{\mathrm{d}t}M_{\alpha\alpha'}^{\sigma\sigma'} = \tfrac{1}{2}e^2\,\mathrm{Tr}\big\{\big[d_{\alpha\sigma}^\dagger A_{\alpha\sigma}^{(-)} - A_{\alpha\sigma}^{(+)}d_{\alpha\sigma}^\dagger\big]N_{\alpha'}^{\sigma'}(t) + \big[d_{\alpha'\sigma'}^\dagger A_{\alpha'\sigma'}^{(-)} - A_{\alpha'\sigma'}^{(+)}d_{\alpha'\sigma'}^\dagger\big]N_\alpha^\sigma(t) + \big[d_{\alpha\sigma}^\dagger A_{\alpha\sigma}^{(-)} + A_{\alpha\sigma}^{(+)}d_{\alpha\sigma}^\dagger\big]\rho_{\rm st}\delta_{\alpha\alpha'}\delta_{\sigma\sigma'} + \mathrm{H.c.}\big\}, \tag{11}$$

where $N_\alpha^\sigma(t)$ can be found from (6) and $\rho_{\rm st}$ is the stationary solution of the master equation (8). In particular, the zero-frequency spin-dependent noise which is of most interest is [6, 10, 19]

$$S_{\alpha\alpha'}^{\sigma\sigma'} = 2\frac{\mathrm{d}}{\mathrm{d}t}\big[M_{\alpha\alpha'}^{\sigma\sigma'}(t) - \bar{I}_\alpha^\sigma\bar{I}_{\alpha'}^{\sigma'}t^2\big]\big|_{t\to\infty}. \tag{12}$$

So far we have outlined a compact formalism for spin-dependent transport through mesoscopic systems. As we will show in the following, this approach can be efficiently used to study the spin-dependent transport phenomena, say, not only the spin-dependent currents, but also their noise properties. The major approximation involved in our formalism is the standard second-order Born approximation with respect to the perturbative expansion of the tunneling Hamiltonian. Apparently, this approach is applicable under the Markov-type condition for relatively high temperatures, say, higher than the tunneling width [33]. In this case, the formalism can be safely applied for arbitrary bias voltages, including those with the Fermi level of the electrode in near-resonance with the energy level of the central (transport) system. Also, the present formalism is applicable to low temperature under large bias voltage, i.e. the electrode's Fermi surface is further away from the central system's energy level than the level broadening. A similar statement also holds for the widely applied rate equation approach at zero temperature [26]. Finally, at low temperature and under low bias voltage (near-resonance transport), an improved self-consistent Born approximation [30] or exact hierarchical equations of motion approach [31] can be satisfactorily employed.

4. Current characteristics

For simplicity, we assume the left and right electrodes have the same spin polarization $p_L = p_R = p$, and the two levels are in resonance, i.e. $E_L = E_R$. This can be achieved, in experiments, by applying appropriate gate voltages on the left and right dots (see, for instance, [32]). Hereafter, we consider a large bias voltage and low temperature in each case, which makes the Fermi functions relevant to the transport processes be either one or zero. Under this condition, electrons only transport in one direction, say, from the left electrode to the right one.

Listed in table 1 are the stationary spin-dependent currents, together with the total charge and spin currents. Numerical results are presented in figure 2, where we further

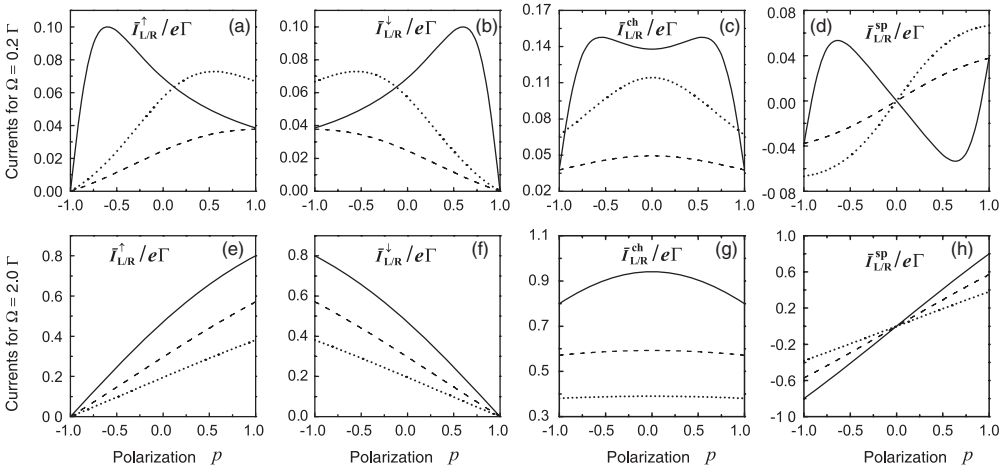

Figure 2. Currents versus spin polarization p for the (i) NINT case (solid curves), (ii) SDCB case (dashed curves) and (iii) DDCB case (dotted curves), respectively. Figures (a)–(d) show, respectively, the spin-up, spin-down, total charge and total spin currents for $\Omega = 0.2\ \Gamma$, and those in (e)–(h) are the corresponding currents for $\Omega = 2.0\ \Gamma$.

assume symmetric coupling, i.e. $\Gamma_{\rm L} = \Gamma_{\rm R} = \Gamma$. Here, the currents are plotted against the spin polarization under the condition of large bias voltage. At finite bias, the energy renormalization will be involved in the present formalism. It arises from the imaginary part of the rate [33] and can be included readily within our theory by the following [34, 35]. The main features found here are summarized as follows: (i) the currents are suppressed in the presence of Coulomb interactions; (ii) there exists a symmetry relation between $\bar{I}^{\uparrow}$ and $\bar{I}^{\downarrow}$, which makes us only need to consider one of them, e.g. $\bar{I}^{\uparrow}$; (iii) the spin-up currents ($\bar{I}^{\uparrow}$) and the total spin currents increase monotonically with p, while the charge currents reach their maxima at $p = 0$.

The results for the noninteracting and weakly coupled dots are shown by the solid curves in figures 2(a)–(d), which differ from the behaviors stated above in (iii). In this weak dot–dot coupling regime, the resultant large occupation probability of the left dot leads to a simple expression for the currents. For instance, the spin-up current in this case can be well approximated by $\bar{I}^{\uparrow} \approx \Gamma_{{\rm L}\uparrow}\rho_{{\rm L}\downarrow}$ with $\rho_{{\rm L}\sigma}$ the probability of the left dot being occupied by a spin-σ electron. As the polarization of the FM electrodes is gradually altered from $p = -1$ to 1, $\rho_{{\rm L}\downarrow}$ decreases rapidly, while $\Gamma_{{\rm L}\uparrow}$ increases linearly. Then, a turnover behavior for the spin-up current is formed as shown by the solid curve in figure 2(a). This is also the basic reason for the unique features of the charge and spin currents shown by the solid curves in figures 2(c) and (d).

5. Noise characteristics

In this section, instead of using the circuit noise [8, 13, 25], we will investigate various fluctuations of spin currents through the left or right junction, i.e. the auto-correlations $S^{\sigma\sigma'}_{\alpha\alpha}$ with $\alpha = {\rm L}$ or R. For the cross-correlations, they simply satisfy the relation $S^{\sigma\sigma'}_{\rm LR} = -S^{\sigma\sigma'}_{\alpha\alpha}$ in the present two-terminal case, as we have checked. It should be noted that, for a three-terminal structure, such a simple relation generally does not take place (see, for instance, [36–38]).

5.1. Self-correlation shot noise

We now turn to the noise characteristics, and first to the self-correlation shot noise. Note that there is a symmetry between $S^{\uparrow\uparrow}_{\alpha\alpha}$ and $S^{\downarrow\downarrow}_{\alpha\alpha}$ with respect to the spin polarization, i.e. figures 3(a) versus (b) and (d) versus (e). Therefore, we need only to consider either $S^{\uparrow\uparrow}_{\alpha\alpha}$ or $S^{\downarrow\downarrow}_{\alpha\alpha}$. For $S^{\uparrow\uparrow}_{\alpha\alpha}$ in figures 3(a) and (d), it is found that both the Coulomb correlation in the dots and the spin polarization of the electrodes will enhance the Fano factor. The shot noise is of NINT < SDCB < DDCB, consistent with the Coulomb correlation strength. The only exception in terms of spin polarization is that shown by the solid curve in figure 3(a), for the weak dot–dot tunnel coupling and in the absence of many-body Coulomb interactions. In this case the Fano factor does not monotonically increase with the polarization degree of the electrodes. This behavior originates from the same reason as that leading to the shoulder behavior of the charge current in figure 2(c).

Remarkably, a profound, strong super-Poisson behavior can be developed by increasing the dot–dot tunnel coupling for both the SDCB and DDCB cases, provided the electrodes are properly spin polarized, see the dashed and dotted curves in figure 3(d). This novel behavior can be understood in terms of the so-called *dynamical spin blockade* mechanism. Take $S^{\uparrow\uparrow}_{\alpha\alpha}$ again for illustration. If the electrode is sufficiently spin-up polarized, the spin-up electrons can more easily pass through the two dots than the spin-down electrons. Furthermore, the SDCB (DDCB) does not allow double occupation in single dot (double dots). Then a mechanism of *fast-to-slow channels* is developed, which results in a bunching behavior and also the super-Poisson statistics of the transport electrons.

Note that the strong Coulomb interaction is essential to the bunching behavior of tunneling events, otherwise the spin-up and spin-down electrons will transport independently, and will not result in the super-Poisson statistics at all [1]. Also, a relatively strong dot–dot coupling is required for the super-Poisson noise in the coupled double-dot system. If the dot–dot coupling is weak, an electron will attempt to stay longer in the left dot. This will weaken the bunching behavior, thus leading

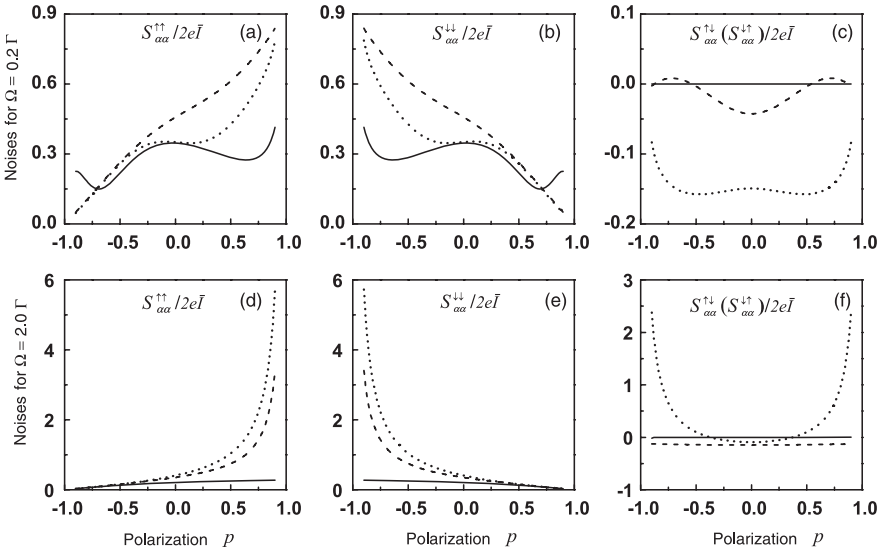

Figure 3. Individual spin-dependent noise for the NINT case (solid curves), SDCB case (dashed curves) and DDCB case (dotted curves), respectively. Figures (a)–(c) are the noises for weak coupling ($\Omega = 0.2\ \Gamma$), and those for strong coupling ($\Omega = 2.0\ \Gamma$) are shown in (d)–(f).

all the noise components to sub-Poisson, see the dashed and dotted curves in figures 3(a) and (b).

The mechanism of dynamic spin blockade also plays an essential role in a three-terminal quantum dot [38, 37] and in an interacting quantum dot with intradot spin-flip scattering connected to FM electrodes [40]. Meanwhile, a similar mechanism called dynamic charge blockade is responsible for the super-Poisson noise in interacting two-channel systems [41–43], as well as double quantum dot structures [44, 45].

5.2. Mutual spin correlation shot noise

We now turn to the mutual spin correlation shot noise ($S^{\uparrow\downarrow}_{\alpha\alpha}$ or $S^{\uparrow\downarrow}_{\alpha\bar{\alpha}}$), which are symmetric to the polarization, as shown in figures 3(c) and (f). For noninteracting dots, the mutual correlation between opposite spin currents is zero, as shown by the solid curves in figures 3(c) and (f). This is simply because the spin-up and spin-down currents are uncorrelated in the absence of Coulomb interaction, despite the electrodes being spin polarized. Similar behavior was also found in [21], where the mutual correlation is zero for noninteracting single dots connected with normal electrodes.

For interacting dots, i.e. the SDCB and DDCB shown in figures 3(c) and (f), the mutual correlation of spin-up and spin-down electrons reveals relatively complex features which can be either *positive* or *negative*. The main features are as follows. (i) For SDCB, negative mutual correlation is found for the weakly coupled dots, if the electrodes are weakly or moderately polarized; but positive correlation can be formed if the electrodes are strongly polarized. (ii) Also for SDCB, the mutual correlation is *fully negative* for strongly coupled dots, independent of the polarization degree of the electrodes. (iii) For DDCB, in the case of weak dot–dot coupling, the mutual correlation is fully negative. (iv) Again for DDCB, but in the case of strong dot–dot coupling, the mutual correlation is positive and can be of strong super-Poissonian for electrodes sufficiently polarized, while it is negative for electrodes weakly or non-polarized.

In this context, we notice that the super-Poissonian self-correlation does not necessarily imply a positive mutual correlation, as shown by the dashed curve in figure 3(f) for the SDCB, where the mutual correlation, despite the polarization degree of the electrodes, is fully negative. A simple and unambiguous understanding for the above positive and negative mutual correlation is yet to be found. It seems more subtle than the super-Poisson statistics of the self-correlation of current.

5.3. Total charge and spin current noises

The total charge and spin current noises are nothing but the combination of those components of the spin-dependent noises, according to (9). The results are displayed in figure 4, where most features such as the sub-Poisson and super-Poisson behaviors can be accordingly understood in terms of the above interpretation of the partial noises.

A noticeable result is the spin current noise resulting from the DDCB. We find that it is constantly Poissonian, regardless of the polarization degree and dot–dot coupling, as shown by the dotted curves in figures 4(b) and (d). Similar Poissonian spin current noise was also found in [21] for a single quantum dot in the Coulomb blockade regime.

To complete this section, we consider all kinds of noises discussed above in the limit of $p = 0$. In this unpolarized situation, simple analytic results can be obtained, as shown in table 2, which serves as a complement to the numerical results in figures 3 and 4. The total charge current noise in the NINT case differs from the ones in [10, 12, 39] by an overall factor of 2 (implied in $\bar{I}_0$, see table 1). This factor originates from the spin degree of freedom, which was ignored there. For interacting cases, under symmetric coupling ($\Gamma_L = \Gamma_R$) and resonant levels ($E_L = E_R$), the total charge current noises are found here to be sub-Poissonian, in either

Table 2. Spin-dependent noise, as well as the total charge and spin current noises for $p = 0$ in different cases.

Noises	$S^{\uparrow\uparrow}_{\alpha\alpha}$ ($S^{\downarrow\downarrow}_{\alpha\alpha}$)	$S^{\uparrow\downarrow}_{\alpha\alpha}$ ($S^{\downarrow\uparrow}_{\alpha\alpha}$)	$S^{\rm ch}_{\alpha\alpha}$	$S^{\rm sp}_{\alpha\alpha}$
Case (i)	$e\bar{I}_0\frac{\Gamma^4-2\Gamma^2\Omega^2+8\Omega^4}{(\Gamma^2+4\Omega^2)^2}$	0	$2e\bar{I}_0\frac{\Gamma^4-2\Gamma^2\Omega^2+8\Omega^4}{(\Gamma^2+4\Omega^2)^2}$	$2e\bar{I}_0\frac{\Gamma^4-2\Gamma^2\Omega^2+8\Omega^4}{(\Gamma^2+4\Omega^2)^2}$
Case (ii)	$e\bar{I}_{\rm s}\frac{9\Gamma^4+14\Gamma^2\Omega^2+28\Omega^4}{9(\Gamma^2+2\Omega^2)^2}$	$-2e\bar{I}_{\rm s}\frac{(11\Gamma^2+4\Omega^2)\Omega^2}{9(\Gamma^2+2\Omega^2)^2}$	$2e\bar{I}_{\rm s}\frac{9\Gamma^4-8\Gamma^2\Omega^2+20\Omega^4}{9(\Gamma^2+2\Omega^2)^2}$	$2e\bar{I}_{\rm s}$
Case (iii)	$e\bar{I}_{\rm d}\frac{\Gamma^4+6\Gamma^2\Omega^2+84\Omega^4}{(\Gamma^2+10\Omega^2)^2}$	$-2e\bar{I}_{\rm d}\frac{(7\Gamma^2+8\Omega^2)\Omega^2}{(\Gamma^2+10\Omega^2)^2}$	$2e\bar{I}_{\rm d}\frac{\Gamma^4-8\Gamma^2\Omega^2+68\Omega^4}{(\Gamma^2+10\Omega^2)^2}$	$2e\bar{I}_{\rm d}$

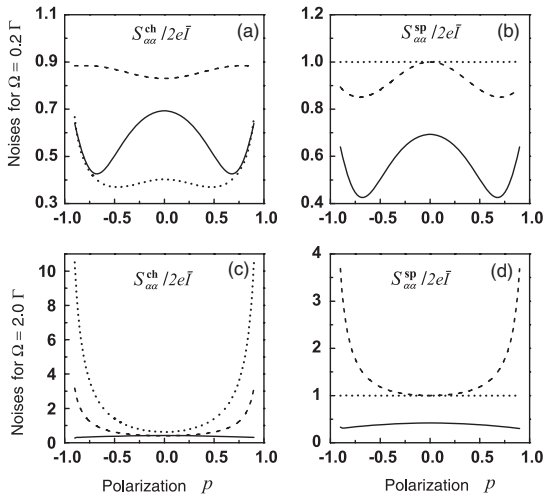

Figure 4. Total charge and spin current noises, obtained by appropriate combination of the individual noise components as shown in figure 3 according to (9). The plot parameters are the same as in figure 3.

the SDCB or the DDCB cases. Very interestingly, however, if $E_{\rm L} \neq E_{\rm R}$ and $\Gamma_{\rm L} > \Gamma_{\rm R}$, the interplay of quantum coherence and the DDCB would develop a dynamical charge blockade mechanism, which then result in a remarkable super-Poissonian noise. Our result in the DDCB case slightly differs from the ones in [44, 10]. Again, the difference arises from the spin degree of freedom, which was neglected in the previous work.

6. Conclusion

To summarize, based on an efficient particle-number-resolved quantum master equation with inclusion of the spin degrees of freedom, we investigated the spin-dependent noises in transport through a pair of coupled quantum dots connected with ferromagnetic electrodes. The modulation of the dot–dot coupling, and the interplay between Coulomb interactions and spin polarization in the electrodes, give rise to rich noise behaviors, such as super-Poissonian, constant Poissonian noises, as well as positive and negative mutual correlations. These unique noise features can serve as additional tools in experiments for revealing the intrinsic dot–dot coupling, as well as the Coulomb interactions involved. The results presented in this work were carried out at zero temperature. At finite temperatures, backward processes are possible, which will in general reduce the current, but enhance the noise, as clearly demonstrated in [43].

Finally, we briefly discuss the measurement of spin-dependent noise. It was shown in [46] that in hybrid ferromagnetic–normal metal structures, the spin current noise exerts a fluctuating spin torque on the magnetization vector, which causes an observable magnetization noise. By measuring this magnetization noise, which has been realized experimentally [47], one then obtains the spin current noise.

Acknowledgments

This work was supported by the RGC (604007) of Hong Kong, the National Natural Science Foundation of China under grant nos. 60425412 and 90503013, and the Major State Basic Research Project under grant no. 2006CB921201.

References

[1] Blanter Y M and Büttiker M 2000 *Phys. Rep.* **336** 1
[2] Nazarov Y V (ed) 2003 *Quantum Noise in Mesoscopic Physics* (Dordrecht: Kluwer)
[3] Blencowe M 2004 *Phys. Rep.* **395** 159
[4] LaHaye M D, Buu O, Camarota B and Schwab K C 2004 *Science* **304** 74
[5] Novotný T, Donarini A, Flindt C and Jauho A P 2004 *Phys. Rev. Lett.* **92** 248302
[6] Flindt C, Novotný T and Jauho A P 2005 *Physica* E **29** 411
[7] Braun M, König J and Martinek J 2006 *Preprint* cond-mat/0601366
[8] Gurvitz S A, Mozyrsky D and Berman G P 2005 *Phys. Rev.* B **72** 205341
[9] Belzig W and Zareyan M 2004 *Phys. Rev.* B **69** 140407(R)
[10] Elattari B and Gurvitz S A 2002 *Phys. Lett.* A **292** 289
[11] Aghassi J, Thielmann A, Hettler M H and Schön G 2006 *Phys. Rev.* B **73** 195323
[12] Sun H B and Milburn G J 1999 *Phys. Rev.* B **59** 10748
[13] Aguado R and Brandes T 2004 *Phys. Rev. Lett.* **92** 206601
[14] Makhlin Y, Schön G and Shnirman A 2001 *Rev. Mod. Phys.* **73** 357
[15] Li X Q, Cui P and Yan Y J 2005 *Phys. Rev. Lett.* **94** 066803
[16] Gurvitz S A, Fedichkin L, Mozyrsky D and Berman G P 2003 *Phys. Rev. Lett.* **91** 066801
[17] Stace T M and Barrett S D 2004 *Phys. Rev. Lett.* **92** 136802
[18] Wang B, Wang J and Guo H 2004 *Phys. Rev.* B **69** 153301
[19] Dong B, Cui H L and Lei X L 2005 *Phys. Rev. Lett.* **94** 066601
[20] Djuric I and Search C P 2006 *Phys. Rev.* B **74** 115327
[21] Sauret O and Feinberg D 2004 *Phys. Rev. Lett.* **92** 106601
[22] Ono K, Austing D G, Tokura Y and Tarucha S 2002 *Science* **297** 1313
[23] McClure D T, DiCarlo L, Zhang Y, Engel H A, Marcus C M, Hanson M P and Gossard A C 2007 *Phys. Rev. Lett.* **98** 056801
[24] Li X Q, Luo J Y, Yang Y G, Cui P and Yan Y J 2005 *Phys. Rev.* B **71** 205304
[25] Luo J Y, Li X Q and Yan Y J 2007 *Phys. Rev.* B **76** 085325
[26] Gurvitz S A and Prager Y S 1996 *Phys. Rev.* B **53** 15932

[27] Yan Y J 1998 *Phys. Rev.* A **58** 2721
[28] MacDonald D K C 1962 *Noise and Fluctuations: an Introduction* (New York: Wiley) chapter 2.2.1
[29] Mozyrsky D, Fedichkin L, Gurvitz S A and Berman G P 2002 *Phys. Rev.* B **66** 161313
[30] Cui P, Li X Q, Shao J S and Yan Y J 2006 *Phys. Lett.* A **357** 449
[31] Jin J S, Welack S, Luo J Y, Li X Q, Cui P, Xu R X and Yan Y J 2007 *J. Chem. Phys.* **126** 134113
[32] Petta J R, Johnson A C, Taylor J M, Laird E A, Yacoby A, Lukin M D, Marcus C M, Hanson M P and Gossard A C 2005 *Science* **309** 2180
[33] Wunsch B, Braun M, König J and Pfannkuche D 2005 *Phys. Rev.* B **72** 205319
[34] Yan Y J and Xu R X 2005 *Annu. Rev. Phys. Chem.* **56** 187
[35] Xu R X and Yan Y J 2002 *J. Chem. Phys.* **116** 9196
[36] Bagrets D A and Nazarov Y V 2003 *Phys. Rev.* B **67** 085316
[37] Cottet A, Belzig W and Bruder C 2004 *Phys. Rev.* B **70** 115315
[38] Cottet A, Belzig W and Bruder C 2004 *Phys. Rev. Lett.* **92** 206801
[39] Kießlich G, Samuelsson P, Wacker A and Schöll E 2006 *Phys. Rev.* B **73** 033312
[40] Djuric I, Dong B and Cui H L 2005 *IEEE Trans. Nanotechnol.* **4** 71
[41] Kießlich G, Sprekeler H and Schöll E 2004 *Semicond. Sci. Technol.* **19** S37
[42] Kießlich G, Wacker A and Schöll E 2003 *Phys. Rev.* B **68** 125320
[43] Wang S K, Jiao H, Li F, Li X Q and Yan Y J 2007 *Phys. Rev.* B **76** 125416
[44] Kießlich G, Schöll E, Brandes T, Hohls F and Haug R J 2007 *Phys. Rev. Lett.* **99** 206602
[45] Sánchez R, Kohler R, Hänggi P and Platero G 2008 *Phys. Rev.* B **77** 035409
[46] Foros J, Brataas A, Tserkovnyak Y and Bauer G E 2005 *Phys. Rev. Lett.* **95** 016601
[47] Covington M, AlHajDarwish M, Ding Y, Gokemeijer N J and Seigler M A 2004 *Phys. Rev.* B **69** 184406